2021 29th Mediterranean Conference on Control and Automation (MED)
June 22-25, 2021. Bari, Puglia, Italy

2021 29th Mediterranean Conference on Control and Automation (MED) | 978-1-6654-2258-1/20/$31.00 ©2021 IEEE | DOI: 10.1109/MED51440.2021.9480226

Forest Fire Risk Prediction from Satellite Data with Convolutional Neural Networks

Alessandro Santopaolo, Syed Saad Saif, Antonio Pietrabissa, *Member*, IEEE and
Alessandro Giuseppi*, *Member*, IEEE

***Abstract*— Forest fires cost the world an estimated value of 200 Billion dollars annually in damages. Furthermore, the main concerns are not only monetary as the vanishment of the carbon-dioxide soaking forests further exacerbates climate change. This paper presents a predictor system based on deep convolutional neural network to predict the risk level of wildfire from satellite data. The proposed Neural Network has an encoder-decoder architecture that allows to provide emergency operators with a pixel-wise fire risk prediction of a given area, allowing precise preventive interventions. The dataset utilised for the training has been generated from publicly available sources as a set of raster images, including several of the most significant satellite products. The paper also proposes a customised loss function for the training of the network and several statistical metrics to establish its performances and validate the reliability of the system. A proof of concept demonstration is discussed for two different case studies: the island of Sicily and an area in California.**

I. Introduction

Forest fires are a crucial and epidemic component of the Earth ecosystem [1]. It is estimated that the mean amount of burned areas caused in the world by fires over the last few years was over 420 Mha, equivalent to an area larger than India [2]. There are multiple causes for forest fire, but unfortunately humans, especially in urban areas, are often the culprits.

In recent years extensive fires are have been raining hugely at any latitude, not only in historical high risk areas as Portugal and Australia but also in new geographical regions as Denmark and Sweden, due to human activities, climate change and industrialization [3].

This work focuses on a case study in the Mediterranean, as in this geographical zone, climate change experts forecast a significant warming and dryness of the soil that will increase the probability of forest fires occurrences and their severity in the next decades [4]. In this regard, Figure 1 reports shown the results of JRC PESETA III Project from [4] regarding a projection of forest fire future risk in Europe as a function of the severity of global warming. For comparison purposes, this paper also reports a case study for an area in California, another area in which fire prevention is of critical importance. The main contributions of this work are:

This work has been partially funded by the ESA Business Application and Space Solution under the 5G for L'ART programme in the scope of the ARIES project (grant agreement No 4000133127).

The authors are with the department of Computer, Control and Management Engineering of the University of Rome La Sapienza, Via Ariosto 25, 00185, Rome, Italy.

* Corresponding Author, email giuseppi@diag.uniroma1.it

- The development of a data-driven solution based entirely on remotely sensed data, gathered from public satellite sources with no need for a ground data-collecting infrastructure to predict the short-term fire risk level of the surveiled area.
- The design of a custom Convolutional Neural Network for the purpose of pixel-wide short-term fire risk prediction.
- The design of new training and evaluation criteria tailored for wildfire predictions.

The rest of the paper is organised as follows: Section II presents some related works available in the literature, while Section III provides a short background on the key concepts regarding CNN and satellite imaging needed to understand the results of the paper; Section IV presents the neural network developed for the system, together with its customised loss function and various evaluation metrics considered. Section VII details the case studies considered in the work, while Section VIII draws the conclusions and highlights future works.

II. Related Works

A. Mathematical and Statistical Models

Several studies have attempted to solve the forest fires prediction problem. In fact, the fire behavior is fundamentally a physico-chemical process representable in principle with dynamical models. As with every modelling process, such representations are subject to assumptions and validity limits, that for complex phenomena such as wildfires significantly impact the quality of their predictions against the real behaviour observed during an emergency situation [6]. A common solution to avoid an extensive model identification process is to utilise empirical and statistical models, able to represent in a simpler, but accurate, way the same underlying phenomena so that they can be combined with physical simulators [7] to help firefighters and emergency operators respond to fires.

Many forest fire risk indexes have been developed by governments and research centers in the last three decades. The heterogeneity of indexes is due to the possibility to let these model rely on many different variables. They differ accordingly to the origin of their variables: meteorological conditions, vegetation conditions or human behaviour.

Regarding weather data, the most famous one is the Fire Weather Index (FWI) [8] developed in 1970. At early stage the FWI technique was related to a standard pine

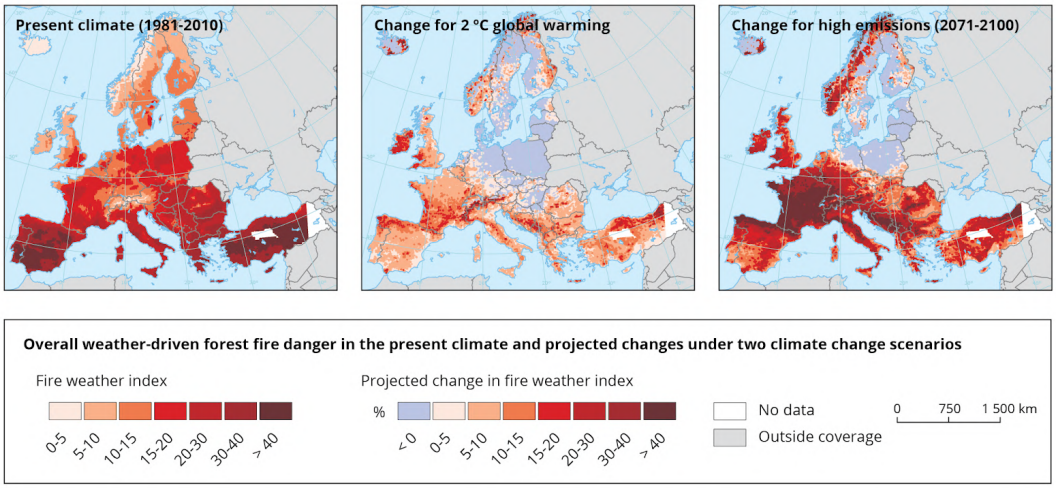

Fig. 1. Effect of global warming on Europe fire season from [5]. (left) current fire risk levels; (center) projected fire risk change for a 2°C increase; (right) projected fire risk change for an high emission scenario.

fuel type and only after a good deal of integration has become the index known nowadays. The six input of this system consists in data related to fuel moisture, fire rate distribution, fuel consumption and fire strength. Each aspect is calculated based on information got from local standard weather readings at noon. Several governments adopted FWI, making it one of the current industry standards.

We mention that conventional weather indexes strongly rely on the position and distribution of the various weather stations and data sources, so that their input has to be interpolated to form a correct spatial map with an appropriate technique [9]. This additional degree of approximation can be easily addressed using remote sensed products as input data, as we propose in this work.

B. Satellite-based data driven solutions

In recent years, remotely sensed products from satellites have become a common data source for the monitoring of the globe, an several satellites now off on board fire detection sensors and solutions. For example, the NASA TERRA and ACQUA satellites [2] employ the MODIS (Moderate Resolution Imaging Spectroradiometer) sensor. Other products of interest are supplied by LANDSAT series satellites that constantly monitor vegetation health and variation.

The quantity and quality of a large number of available data and the technological advancement of the last decade have led many researchers to focus their attention on a data-centric approach to fire prediction. In fact, the use of artificial intelligence techniques and, in particular, machine learning is especially relevant for the type of data available, as ML techniques have demonstrated the potential to produce better outcomes for the spatial prediction of wildfires compared to conventional statistical methods [10].

The most used ML methods used for wildfire management are artificial neural networks [11]–[13], but we also mention some studies utilising kernel logistic regression (KLR) [14], support vector machine (SVM) [15] and random forests (RF) [16], [17]. Even though the mentioned solution have shown good performances and have been used and studied, these ML techniques are not the state-of-the-art for image analysis, as they do not exploit the spatiality of the information contained in satellite images and also require a feature extraction process, that can be avoided with Deep Learning.

Among Deep Learning architectures, Convolutional Neural Networks (CNN) [18] in particular allow the seamless analysis of imaging data, enabling also pixel-wise localisation of fires/patterns of interest to further enhance the precision of their analysis. The most recent CNN architectures also do not require any feature extraction process and are hence able to operate on the raw imaging data.

III. Background on Deep Learning and Satellite Imaging

A. Deep Learning and Convolutional Neural Networks

Artificial Neural Networks (NN) are a class of functional approximators that gathered an unprecedented attention in the research community for their capabilities to deal with complex problems and their generalisation capabilities. In general, NN are constituted by a series of *layers* containing several *neurons*. The network is said to be *trained* on some data following a procedure known as *backpropagation* that updates the network (and in particular its *weights*) to approximate some function that links the input and output data. Convolutional Neural Networks are a special class of Neural Networks in which each neuron has a locally limited connectivity with the previous layer [18], allowing the deployment of significantly deeper models while keeping the number of trainable parameters limited. The local connectivity of neurons that characterises CNN is also exploited to easily localise spatially relevant patterns (e.g. faces in a photograph, objects in a background, ...), making them an ideal tool for image analytics and in particular fire risk predictions.

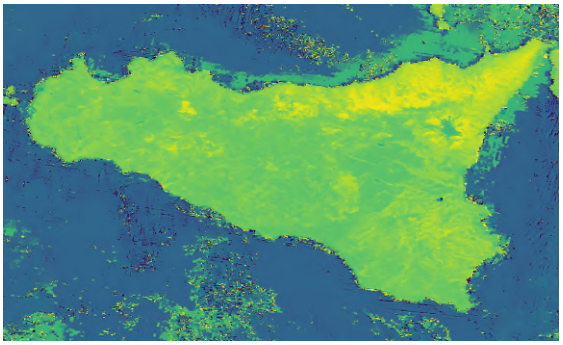

Fig. 2. Example of NDVI raster image

Fig. 3. Example of Terra MODIS surface reflectance measurement from the MOD09A1 product

B. Satellite imaging

In this work, MODIS (or Moderate Resolution Imaging Spectroradiometer) satellite products have been used. MODIS is a key instrument aboard the TERRA and AQUA satellites and has been very important for terrestrial satellite analysis, especially regarding climate change.

In this study, in order to predict future fires a total of six geo-environmental and climate variables has been considered and described in the following subsections.

C. NDVI and NDWI

Common remote-sensing vegetation indices utilised to monitor the distribution and health of plants are the NDVI and NDWI. In fact, we have to consider for fire risk prediction that the vegetation structure and stress are correlated with their moisture content which in turn influences forest fire ignition and growth.

The remote monitoring of vegetation is possible since it absorbs and re-emits a different percentage of solar radiation in different bands, i.e. in different frequency ranges and wavelengths. In particular, the percentage of re-emitted radiation in specific bands, such as near-infrared (NIR), red (RED) and short-wave infrared (SWIR), indicates plant health or water stress, and vegetation indices are a combination of the percentage of radiation reflected in a set of specific bands. In order to calculate those indices the MODIS product MOD09A1 v006 has been used, as it provides an estimate of the surface spectral reflectance of Terra MODIS Bands 1 through 7. It offers seven bands with a spatial resolution of 500 meters.

The most used vegetation index is undoubtedly the Normalized Difference Vegetation Index (NDVI): it describes the vigor level of the crop and is calculated as the ratio between the difference and the sum of the radiations reflected in the near infrared and in the red.

$$NDVI = \frac{(REF_{nir} - REF_{red})}{(REF_{nir} + REF_{red})} \quad (1)$$

Where REF_{nir} and REF_{red} are the spectral reflectances measured in the near infrared and in the visible (red) wavebands. The interpretation of the absolute value of the NDVI is highly informative, since it allows you to immediately recognize the areas of the company or field that have development problems. The NDVI is a simple index to interpret. The values can vary between -1 and 1, but those between -1 and 0 are typical of non-cultivated areas such as waterways and anthropogenic areas. A sample image reporting NDVI for the island of Sicily is shown in Figure 2.

Another vegetation index to take into account is the Normalized Difference Water Index (NDWI) that is used to assess presence of moisture in plants. It represents the normalized Difference Water Index and was introduced for the first time in 1996 and incorporate information about humidity in soils and plants. It is calculated as:

$$NDWI = \frac{(REF_{nir} - REF_{swir})}{(REF_{nir} + REF_{swir})} \quad (2)$$

Where REF_{swir} is the spectral reflectance measured in the short-wave infrared wavebands. NDWI is less sensitive to atmospheric effects than NDVI [19]. Low values are synonymous of water stress, whereas high values represent adequate moisture content. Figure 3 reports an example of reflectance measuring from MOD09A1.

D. TRMM

A daily accumulated rainfall product is deduced by the NASA product 3-H TRMM Multi-Satellite Precipitation Analysis (3B42) in mm/day (TRMM) [20]. In order to achieve the data for a day, a summation of pixel values in a grid cell is applied [21]. The temporal resolution of the product is one day with a spatial resolution of $0.25° \times 0.25°$. The Mission carried out to obtain this product was the Tropical Rainfall Measuring Mission Project, and example of a TRMM product is reported in Figure 4.

E. Land surface temperature

For fire prediction, the temperature may be considered one of the most critical values to take into account. The Land Surface temperature (LST) is included in the MOD11A2 package, with a temporal resolution of 8 days, the same as the TERRA and ACQUA satellites. This product offers an average 8-day LST for each pixel, with a spatial resolution of one square kilometer [23]. Figure 5 reports an example of an image from such product.

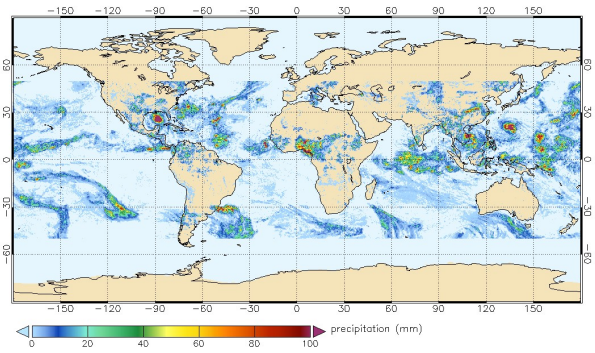

Fig. 4. Example of TRMM product [22]

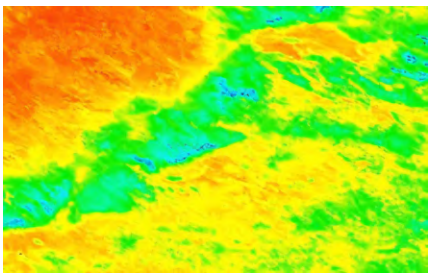

Fig. 5. Example of land surface temperature raster image [24]

F. Land cover type

Land cover map are the basis for the number of applications in the environmental and agricultural-forestry fields: the forest, the fires, the irrigated areas, the crops and the different uses of the land can be identified in order to produce maps that support the professionals in the management and oversee of a territory. The study of the evolution of land use, represents and highlights the characteristics of the area of interest. The product utilised in this study is the MCD12Q1 [25] package. It offers a temporal resolution of one year and is active since 2001, with a spatial resolution of 500 square meters in a 1200 by 1200 km grid. In this work, the layers Type 1 of the product has been used for land cover classification, as it is defined by the International Geosphere-Biosphere Programme (IGBP) and has 17 land cover classes, such as water, urban, croplands, savannas, snow and ice, barren lands, and five types of forests. An example of such imaging is reported in Figure 6.

G. Digital elevation model

The Digital Elevation Model (DEM) is a variable related to the topography. We decided to include it in this study because it affects the presence and number of human and animal species in a given area. Furthermore, its relevance to the occurrence of fire in literature has been demonstrated by several studies such as [26]. The product comes from the NASADEMHGT dataset satellite package, that was obtained by the NASA shuttle during the SRTM mission and collected with Radar interferometry. NASADEM is segmented into $1^\circ \times 1^\circ$ tiles and consists of all land between 60° N and

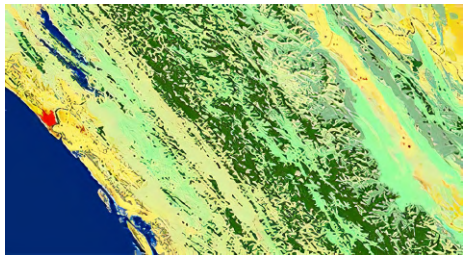

Fig. 6. Example of land cover raster image

Fig. 7. Example of DEM raster image

56° S, accounting for about 80% of the Earth's total land mass with a resolution of 30m [27]. The Figure 7 shows a DEM image.

H. fire-mask

NASA MYD14A2 is the satellite product used to provide a map of acting fires [28]. The product fire-mask is used as our ground truth for forecasting fire risk rating, so that the network output is trained against this image, as our objective is to determine fire-masks prediction (for the upcoming days) starting from the other six satellite products. This product has a spatial resolution of 1 kilometer and a temporal resolution of 8 days. The value of each pixel is the highest fire value observed during the eight-day period (between 0 and 9). The mask is determined by synthesizing the absolute detection of fire and the relative background. The SDS layer includes a fire-mask with ten values representing ten different situations . An example of a fire-mask is depicted, for the entire island of Sicily, in Figure 8.

Fig. 8. Example of fire-mask raster image, Sicily, scale of Greys

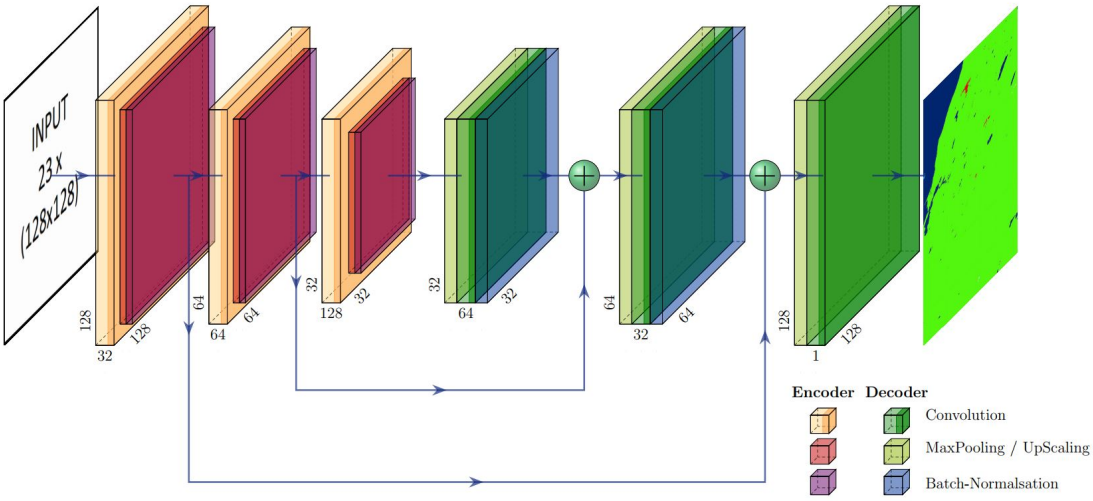

Fig. 9. Example of encoder-decoder CNN architecture

I. Raw data collection

All the mentioned satellite products were downloaded from the respective sources using the EarthData search engine [29]. The dataset used in the experiment consist of the satellite products mentioned for the year 2019.

J. Data Augumentation and windows size

To performe a data augmentation, we subsample random regions of size 128X128 pixels and then check if the sampled data meets certain conditions. The conditions are placed to make sure that the data input is representative of the area and problem of interest. For instance, we check the image for the percentage forest fires as well as the percentage of water in the area. The forest fire test is there to ensure that the regions that have no fire are not included, since these regions do not contain any data on which to extrapolate the fire probabilities. The water test similarly is also there to ensure that the regions does not contain too much water as obviously we are not interested in finding the fire probabilities in that region. In this way we assist the network to better perform the inferring process providing high significant training images.

K. Adding data from the previous year

The input data built up to this stage does not consider historical fires. In order to give the network other instrument to well perform the fire prediction we insert fire data of previous year. In particular we add another image obtained averaging the fire-mask of the considered area over the entirety of the previous year. This new image allows to better predict human-related fires, as the periodic burns performed by farmers for their cultures.

IV. Proposed Convolutional Neural Network for Fire Risk Prediction

The proposed CNN architecture is based on the encoder-decoder architecture typical of autoencoders. This kind of architecture is suitable for this analysis because the output produced by the network is an image itself, and can be trained to predicts the pixel level fire risk in the form of a fire-mask.

The structure of this kind of networks presents a bottleneck in the middle, as depicted in Figure 9. We can think at the network as constituted by two different compoents.

In the first part, the encoder reduces the dimensionality of our data focusing on the most relevant features for the regression task (i.e. on very specific relevant features of the images that are used to better predict level of fires).

In the second part of the network, we find an almost mirrored architecture, with the output fire-mask produced by merging the relevant information from the previous layers and the bottleneck layer.

The network we deployed is composed by 6 convolutional layers respectively having 32, 64, 128, 64, 32 and 1 kernels, all of them having an uniform kernel size of 3×3 and padding set to 'same' with a stride of 2. Each convolution layer is followed by an activation function (ReLU) and a 2×2 max-pooling layer. In the last convolutional layer the activation function was set to be a sigmoid, allowing a better scaling in the appropriate range to produce the fire-mask. After each convolutional layer a batch normalization has been used to increase the stability of the network training and its generalisation properties. The network was implemented utilising Keras.

V. Loss function design

The loss function has to be carefully designed in any machine-learning tasks so that its numerical value should reflect the quality of the produced output, capturing the goals and performance of the neural network that is being trained.

The task considered in this study consists in a regression problem, so we employed a Regressive Loss Functions (RLF). In the literature there are different variants of RLF, as for example the Square Error Loss, the Absolute Error Loss and the Smooth Absolute Error.

In this study we have deviated from such standard solutions, as the commonly employed pixel-wise mean squared

error (MSE) (evaluated between the provided fire-mask and the one predicted by the neural network) does not satisfy our goals. The reason for that is due to the fact that the percentage of fire-critical areas is very small, as most of the area does not have a significant fire risk level. So, with the standard MSE even if the network completely fails to predict the fire, the network is still able to obtain a very limited loss value, converging consequently to a local minimum.

For these reasons, we modified the pixel-wise MSE loss to give more weight to the region where there is a fire risk, or, in other words, drastically penalize the system when a fire is not well classified. The steps necessary to calculate such a loss function are then:

1) Create a weight mask from the ground truth (output label) for each data sample in the dataset. The fire region is associated to more weight (10 times in our settings).
2) Calculate the pixel-wise squared difference between the label and a prediction generated by the network during training.
3) Multiply the weight mask with the squared difference to get the weighted squared difference.
4) Average over all pixels the weighted difference obtained.

A. Performance evaluation

The evaluation criteria are a crucial element in assessing the prediction performance and guiding the classifier modeling [30]. Precision and recall are two indicators used in machine learning to evaluate the quality of a decision model or predictive model. In particular they are used in classification tasks when the dataset is unbalanced. Even if our problem was formulated as a regression task, seeing every single pixel as an entry to be classified allows the usage of such metrics. A problem that arises is the presence in our case of a huge number of negative samples (no fire zone) makes the most used metrics, the accuracy, not informative.

Precision is the ratio of the number of correct predictions of an event (class) to the total number of times the model predicts it. When a model is accurate for a class, it rarely fails whenever it predicts the event. However, false negatives could be common even if the model is precise. For example, in our case, if the system does not predict a fire (i.e. a false negative), the model does not lose score in precision.

Recall on the other hand measures the sensitivity of the model, as it is the ratio between the correct predictions for a class over the total of cases in which it actually occurs. When a model is sensitive to a class, it predicts it every time it occurs. However, it could predict it even when it doesn't happen (i.e., false positives could be many).

In order to calculate these statistical measures, we need to define for our problem the concepts of True Positive, False Positive and False Negative values. This is not a straightforward task on images, as our problem was formulated as a regression task whereas these concepts were introduced for classification.

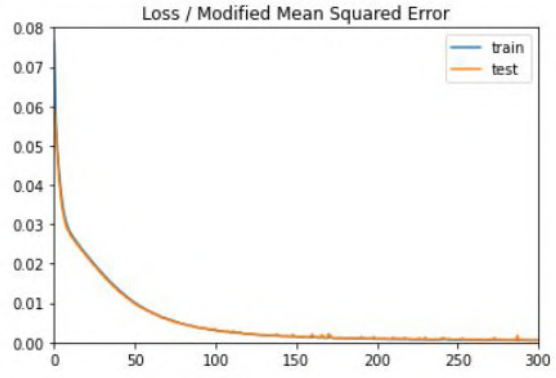

Fig. 10. Trainig and Test loss

We designed a procedure that simplifies the classification of a portion of the image as true or negative sample as follows:

1) Define a threshold radius (30px in our settings) as a fixed quantity related to the desired granularity of the model prediction.
2) Take a fire in the label and see if there is a predicted fire (in the netowrk's output) inside a circle of the above mentioned radius. If the fire is indeed predicted, then we count this as a true positive else, it is classified as a false negative.
3) Apply this procedure for all the fires in the label. If there are any fires remaining in the prediction that are not accounted for in the previous steps, they are considered false positives.

Once we have these numbers, we can calculate the precision and recall using the formulas given below:

$$\text{Precision} = \frac{\text{True Positives}}{\text{True Positives} + \text{False Positives}} \tag{3}$$

$$\text{Recall} = \frac{\text{True Positives}}{\text{False Negatives} + \text{True Positives}} \tag{4}$$

providing a reasonable performance index that is tailored to our specific application.

VI. Input and Output of the Neural Network

The input of the network is then constituted by: (i) 6 satellite products (NDVI, NDWI, TRMM, Temperature during the day, Temperature during the day, firemask) averaged during the past 8 days; (ii) the same quantities as in (i) but averaged over the 8 days before; (iii) the same quantities as in (ii) but averaged over the 8 days before; (iv) An image regarding land cover type and one DEM image; (v) the average firemask of the zone, evaluated over the entirety of the previous (2019) year; (vi) two images that encode the x and y geographical coordinates of the area, as in [16].

As mentioned, the output of the network is the predicted average firemask for the incoming 8 days.

Figure 10 reports the training results in terms of loss convergence for the island of Sicily (similar results were observed for the other case study).

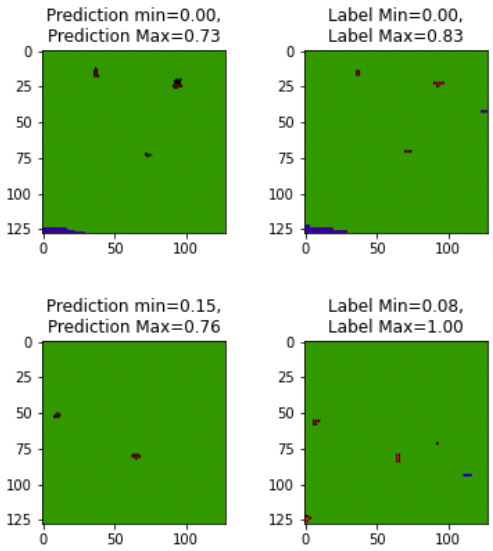

Fig. 11. Comparison between predicted (right) and label (left) risk map of two Sicily zones

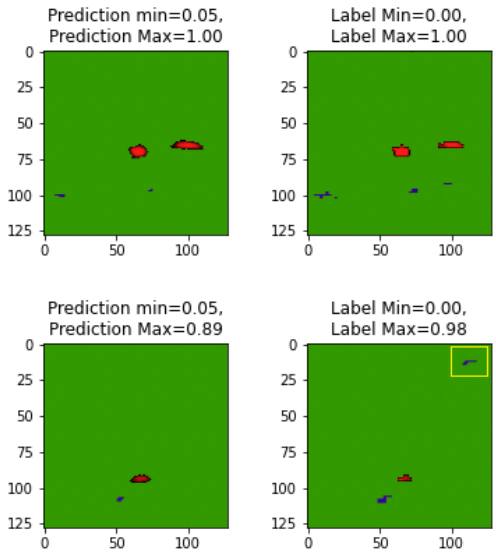

Fig. 12. Comparison between predicted (right) and label (left) risk map of two LA County zones

VII. Case Studies

In this study we considered as a case study the island of Sicily, in which the problem of forest fires is particularly serious, due to the set of socioeconomic factors which make the territory particularly fragile with regard to this phenomenon. These factors can be summarized as follows: climatic conditions as the long spring-summer drought, low atmospheric humidity, high temperatures and the accentuated windiness, excessive anthropogenic pressure in some parts of the territory and the abandonment of mountain areas [31].

To validate the developed tool on another, very different, area, we also considered an area around Los Angeles City. A significant number of forests is present in this zone and in recent years it was subject to a significant number of fires.

The trained network is able to recognize zones with high risk possibility of fire. The parameter that we consider most significant in the study is the recall since it is related to the number of false negatives, as any missing prediction can cost a huge amount of money and cause severe damages. In the case of false positive instead, there are only problems related to firefighters' management activities. In fact, The need to improve the recall value has been the key factor in the development of the customized loss function.

In each of the Figures 11, 12 we report two typical output of the network compared with the correct fire-masks from the satellite product, obtained for input data outside of the training dataset. We note that the quality of the prediction is overall very good, with some minor fires that were unpredicted in the Sicily case. In the LA scenario, only a single zone with an high fire risk in the predictions (highlighted with a yellow box) was missed, but that are geographical corresponded to a highly populated area near San Bernardino City, so the concentration of human activities probably contributed to this fire.

Even if the results for the island of Sicily are satisfactory, out system performed better in the Los Angeles area. We supposed this is due to two factors: land cover and human behaviour. The data we fed into the CNN are mostly related to the weather and the vegetation characteristics of the observed land, so the network does not perform well when external events are the fire cause, as in the case of human behaviour. In Sicily, this problem is very limiting because the amount of forest fires caused by environmental factors is statistically irrelevant with respect human fires [32].

In general, predicting when humans cause a fire (in a voluntary or accidentally way) is a difficult task. We tried to solve this issue looking at the statistics about fires causes. The Civil Protection [31] uphold that the first cause of arsons is the renewal of the pasture that is a cyclical phenomenon. We observed that with the inclusion of the average, pixel-wise, fire risk evaluated over the previous year significantly improved the prediction in the island of Sicily, hinting at a probable better prediction of such periodic burns.

Furthermore, that the lower performances in Sicily are also probably due to the land cover type, as the network relies on vegetation data it is not surprising to see that its overall performances decrease if the number of forest is low. According to the data reported in the current fire prevention plan of the Italian Civil Protection, the wooded area in Sicily is only about 11% of the territorial surface [31]. The presence of a several urban area further decreases the average performance in this territory, because the network can be disoriented in this context due to human-related fires. This hypothesis is validate by evaluating the results of the network only in forest zone, which improve of about 7%.

If we look at literature results, the performances obtained in this study overtake the ones achieved by two relevant results in the field of AI-based fire risk prediction from

satellite products. For a coherent comparison we discuss only the algorithms with a similar dataset structure and selection of remote sensing products, namely [16] and [33]. These two studies got a MSE of respectively 0.7 and 0.00285 while the higher result in this study is 0.0002. Indeed, the chosen network architecture combined with a customized loss function is more efficient than a simple ANN or a random forest algorithm to accomplish forest fire prediction. This can be explained looking at the structure of the dataset that well combines spatial and temporal resolution in the network analysis and at the peculiarities of CNN model tailored at analysing adjacent spatial information.

VIII. Conclusions and future works

In this paper we presented a predictor system able to obtain a short-term (8 days) prediction of fire risk from remotely sensed satellite imaging data. To this end, we designed a convolutional neural network with a customised loss function that was trained on six different satellite products. The trained system obtains very precise prediction in both case studies (the island of Sicily and an area in California). Future works are related to the inclusion of more satellite products to improve the predictions and in developing a new network architecture able to generalise better on new areas.

References

[1] W. J. Bond and J. E. Keeley, "Fire as a global 'herbivore': the ecology and evolution of flammable ecosystems," *Trends in ecology & evolution*, vol. 20, no. 7, pp. 387–394, 2005.

[2] L. Giglio, L. Boschetti, D. P. Roy, M. L. Humber, and C. O. Justice, "The collection 6 MODIS burned area mapping algorithm and product," *Remote Sensing of Environment*, vol. 217, pp. 72–85, Nov. 2018.

[3] M. A. Crimmins, "Synoptic climatology of extreme fire-weather conditions across the southwest united states," *International Journal of Climatology: A Journal of the Royal Meteorological Society*, vol. 26, no. 8, pp. 1001–1016, 2006.

[4] C. C. EEA, "Impacts and vulnerability in europe 2016–an indicator-based report," *Luxembourg: Publications Office of the European Union*, vol. 1, p. 2017, 2017.

[5] E. C. J. R. Centre., *Forest fire danger extremes in Europe under climate change: variability and uncertainty.* Publications Office, 2017.

[6] H. C. M., "Evaluating crown fire rate of spread predictions from physics-based models," *Fire Technology 52.1: 221-237*, 2016.

[7] A. Sullivan, "A review of wildland fire spread modelling, 1990-present 3: Mathematical analogues and simulation models," *arXiv preprint arXiv:0706.4130*, 2007.

[8] B. J. Stocks, T. Lynham, B. Lawson, M. Alexander, C. V. Wagner, R. McAlpine, and D. Dube, "Canadian forest fire danger rating system: an overview," *The Forestry Chronicle*, vol. 65, no. 4, pp. 258–265, 1989.

[9] P. A. Longley, M. F. Goodchild, D. J. Maguire, and D. W. Rhind, *Geographic information systems and science*. John Wiley & Sons, 2005.

[10] A. B. Massada, A. D. Syphard, S. I. Stewart, and V. C. Radeloff, "Wildfire ignition-distribution modelling: a comparative study in the huron–manistee national forest, michigan, usa," *International journal of wildland fire*, vol. 22, no. 2, pp. 174–183, 2013.

[11] L. A. Dimuccio, R. Ferreira, L. Cunha, and A. C. de Almeida, "Regional forest-fire susceptibility analysis in central portugal using a probabilistic ratings procedure and artificial neural network weights assignment," *International Journal of Wildland Fire*, vol. 20, no. 6, pp. 776–791, 2011.

[12] O. Satir, S. Berberoglu, and C. Donmez, "Mapping regional forest fire probability using artificial neural network model in a mediterranean forest ecosystem," *Geomatics, Natural Hazards and Risk*, vol. 7, no. 5, pp. 1645–1658, 2016.

[13] D. M. Debinski, "Forest fragmentation and matrix effects: the matrix does matter," *Journal of Biogeography*, vol. 33, no. 10, pp. 1791–1792, 2006.

[14] H. Hong, B. Pradhan, C. Xu, and D. T. Bui, "Spatial prediction of landslide hazard at the yihuang area (china) using two-class kernel logistic regression, alternating decision tree and support vector machines," *Catena*, vol. 133, pp. 266–281, 2015.

[15] H. Hong, P. Tsangaratos, I. Ilia, J. Liu, A.-X. Zhu, and C. Xu, "Applying genetic algorithms to set the optimal combination of forest fire related variables and model forest fire susceptibility based on data mining models. the case of dayu county, china," *Science of the total environment*, vol. 630, pp. 1044–1056, 2018.

[16] B. Yu, F. Chen, B. Li, L. Wang, and M. Wu, "Fire risk prediction using remote sensed products: A case of cambodia," *Photogrammetric Engineering & Remote Sensing*, vol. 83, no. 1, pp. 19–25, 2017.

[17] H. Hong, H. R. Pourghasemi, and Z. S. Pourtaghi, "Landslide susceptibility assessment in lianhua county (china): a comparison between a random forest data mining technique and bivariate and multivariate statistical models," *Geomorphology*, vol. 259, pp. 105–118, 2016.

[18] A. Khan, A. Sohail, U. Zahoora, and A. S. Qureshi, "A survey of the recent architectures of deep convolutional neural networks," *Artificial Intelligence Review*, vol. 53, no. 8, pp. 5455–5516, Apr. 2020. [Online]. Available: https://doi.org/10.1007/s10462-020-09825-6

[19] B.-C. Gao, "Ndwi—a normalized difference water index for remote sensing of vegetation liquid water from space," *Remote sensing of environment*, vol. 58, no. 3, pp. 257–266, 1996.

[20] G. J. Huffman, R. F. Adler, D. T. Bolvin, and E. J. Nelkin, "The trmm multi-satellite precipitation analysis (tmpa)," in *Satellite rainfall applications for surface hydrology*. Springer, 2010, pp. 3–22.

[21] G. Huffman, D. Bolvin, E. Nelkin, and E. Stocker, "Gpm (imerg) late precipitation l3 1 day 0.1 degree 3 0.1 degree v03," *Goddard Earth Sciences Data and Information Services Center (GES DISC). Accessed: April*, vol. 20, p. 2017, 2016.

[22] G. E. S. Data and I. S. Center. Trmm-3b42-daily. [Online]. Available: https://disc.gsfc.nasa.gov/datasets/TRMM_3B42_Daily_7/summary

[23] Z. Wan, S. Hook, and G. Hulley, "Mod11a2 modis/terra land surface temperature/emissivity 8-day l3 global 1km sin grid v006," *NASA EOSDIS Land Processes DAAC*, vol. 10, 2015.

[24] N. EOSDIS. Mod11a2v006. [Online]. Available: https://lpdaac.usgs.gov/products/mod11a2v006/

[25] M. Friedl and D. Sulla-Menashe, "Mcd12q1 modis/terra+ aqua land cover type yearly l3 global 500m sin grid v006. 2019, distributed by nasa eosdis land processes daac."

[26] G. Zhang, M. Wang, and K. Liu, "Forest fire susceptibility modeling using a convolutional neural network for yunnan province of china," *International Journal of Disaster Risk Science*, vol. 10, no. 3, pp. 386–403, 2019.

[27] NASA JPL, "Nasadem merged dem global 1 arc second v001," 2020. [Online]. Available: https://lpdaac.usgs.gov/products/nasadem_hgtv001

[28] L. Giglio and C. Justice, "Myd14a2 modis/aqua thermal anomalies/fire 8-day l3 global 1km sin grid v006," 2015. [Online]. Available: https://lpdaac.usgs.gov/products/myd14a2v006/

[29] NASA. Earthdata engine. [Online]. Available: https://search.earthdata.nasa.gov/search

[30] M. Sokolova and G. Lapalme, "A systematic analysis of performance measures for classification tasks," *Information processing & management*, vol. 45, no. 4, pp. 427–437, 2009.

[31] I. Sciortino and A. Ganci, "Cause dolose e colpose degli incendi in sicilia: proposte per la rimozione degli interessi e dei bisogni alla base del fenomeno," *Atti del convegno su "Incendi boschivi e rurali in Sardegna"(Cagliari14-16 maggio 2004), Regione Autonoma della Sardegna, Assessorato della Difesa dell'Ambiente, Corpo Forestale e di vigilanza ambientale*, pp. 177–185, 2005.

[32] K. C. Short, "Spatial wildfire occurrence data for the united states, 1992-2015 [FPA_FOD_20170508] (4th edition)." [Online]. Available: 10.2737/rds-2013-0009.4

[33] E. E. Maeda, A. R. Formaggio, Y. E. Shimabukuro, G. F. B. Arcoverde, and M. C. Hansen, "Predicting forest fire in the brazilian amazon using modis imagery and artificial neural networks," *International Journal of Applied Earth Observation and Geoinformation*, vol. 11, no. 4, pp. 265–272, 2009.